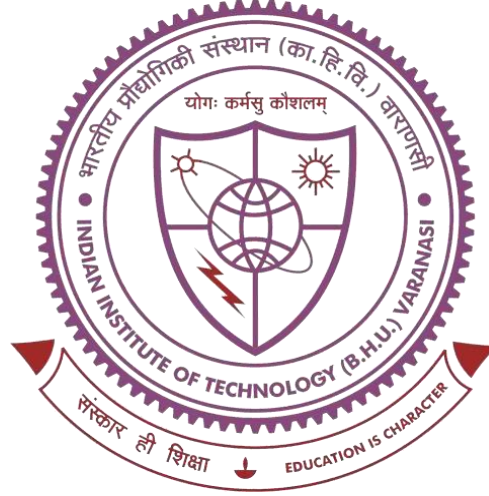


Lanthanide-doped optical materials for temperature sensing and latent fingerprint detection



Thesis submitted in partial
fulfilment For the Award of Degree

DOCTOR OF PHILOSOPHY

In

Physics

By

Sachin Singh

Department of Physics
INDIAN INSTITUTE OF TECHNOLOGY
(BANARAS HINDU UNIVERSITY)
VARANASI- 221005

Roll No: 19171026

2024

Dedicated

to

*My parents,
brothers, sisters,
wife, son,
teachers and
well wishers*

Department of Physics
INDIAN INSTITUTE OF TECHNOLOGY
(BANARAS HINDU UNIVERSITY)
VARANASI - 221005



CERTIFICATE

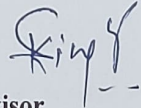
It is certified that the work contained in the thesis titled " **Lanthanide-doped optical material for temperature sensing and latent fingerprint detection** " by "Mr. Sachin Singh" (Roll No. 19171026) in partial fulfilment of the requirement for award of the degree of **Doctor of Philosophy** at **Indian Institute of Technology (BHU), Varanasi** is a record of his own work carried out under my supervision and guidance and this work has not been submitted elsewhere for a degree.

It is further certified that the student has fulfilled all the requirements of Comprehensive Examination, Candidacy, and SOTA for the award of Ph.D. Degree.

Date: 26.12.2024

Place: Varanasi

Supervisor


(Dr. Sunil Kumar Singh)
Department of Physics
Indian Institute of Technology
(Banaras Hindu University)
Varanasi (U.P.) 221005
Assistant Professor
Department of Physics
Indian Institute of Technology
(Banaras Hindu University)
Varanasi-221005

DECLARATION BY THE CANDIDATE

I, "Sachin Singh" (Roll No. 19171026), certify that the work embodied in this thesis is my own bonafide work and carried out by me under the supervision of "Dr. Sunil Kumar Singh" from July 2019 to December 2024, at the Department of Physics, Indian Institute of Technology (Banaras Hindu University), Varanasi. The matter embodied in this thesis has not been submitted for the award of any other degree/diploma. I declare that I have faithfully acknowledged and given credits to the research workers wherever their works have been cited in my work in this thesis. I further declare that I have not willfully copied any others work, paragraphs, text, data, results, etc., reported in journals, books, magazines, reports dissertations, thesis, etc., or available at websites and have not included them in this thesis and have not cited as my own work.

Date: 26.12.2024

Place: Varanasi



Signature of the Student

(Mr. Sachin Singh)

CERTIFICATE BY THE SUPERVISOR

It is certified that the above statement made by the student is correct to the best of my knowledge.



Dr. Sunil Kumar Singh
(Supervisor)
Department of Physics
Indian Institute of Technology
(Banaras Hindu University)
Varanasi
Assistant Professor
Department of Physics
Indian Institute of Technology
(Banaras Hindu University)
Varanasi-221005



Prof. Sandip Chatterjee
(Head of Department)
Department of Physics
Indian Institute of Technology
(Banaras Hindu University)
Varanasi
HEAD/विभागाध्यक्ष
भौतिकी विभाग/Dept. of Physics
भा०प्रौ०सं०/(का०हि०वि०)/IIT (BHU)
वाराणसी/Varanasi-221005

COPYRIGHT TRANSFER CERTIFICATE

Title of the Thesis: **“Lanthanide-doped optical material for temperature sensing and latent fingerprint detection”**


Name of the Student: **Mr. Sachin Singh**

Copyright Transfer

The undersigned hereby assigns to the Indian Institute of Technology (Banaras Hindu University) Varanasi all rights under copyright that may exist in and for the above thesis submitted for the award of the **“Doctor of Philosophy”** degree in **Physics**.

Date: 26.12.2024

Place: IIT (BHU) Varanasi


Signature of the Student
(Mr. Sachin Singh)

Note: However, the author may reproduce or authorize others to reproduce material extracted verbatim from the thesis or derivative of the thesis for author's personal use provided that the source and the Institute's copyright notice are indicated.

ACKNOWLEDGEMENTS

Foremost, I would like to express my love to my parent for their care, support, and pure love in my academic journey. I really appreciate my dearest wife for her patience, support, care and true love for me and believing in me throughout this journey. I would like to express my sincere gratitude to my supervisor Dr. Sunil Kumar Singh, Department of Physics, Indian Institute of Technology (Banaras Hindu University), Varanasi for his continuous support and guidance in my research work, for his motivation, enthusiasm, and immense knowledge.

I would also like to express my sincere thanks to RPEC member's Prof. Avanish Singh Parmar, Department of Physics, and Dr. Akhilesh Kumar Singh, School of Materials Science & Technology, Indian Institute of Technology (Banaras Hindu University), Varanasi for their encouragement, insightful comments, and stimulating me in this journey.

I would like to thank Dr. Akhilesh Kumar Singh, Department of Physics, Banasthali Vidyapith, Rajasthan for collaborative research work and solving the scientific difficulties faced during the research work. I am also thankful to Prof. Vineet Kumar Rai, Department of Physics, Indian Institute of Technology (ISM) Dhanbad, Jharkhand for providing his lab facility in temperature sensing application.

I wish to express deep regards to all the teachers of the Department, Prof. Sandip Chatterjee, Prof. Deba Prasad Giri, Prof. Prabhakar Singh, Prof. Rajendra Prasad, Prof. Abhishek Kumar Srivastava, Prof. Praveen Chandra Pandey, Prof. Shail Upadhyay, Dr. Anita Mohan, Dr. Avanish Singh Parmar, Dr. Shradha Mishra, Dr. Saurabh Tripathi, Dr. Sunil Kumar Mishra, Dr. Swapnil Patil, Dr. Awaneesh Singh, Dr. Gauhar Abbas, Dr. Rajeev Singh, Dr. Somnath Nag, Dr. Bidya Binay Karak, Dr. Pawan Kumar Aluri, Dr. Prasun Dutta, Dr. Biswanath Bhoi, Dr. Kuldeep Verma for their direct or indirect support for my progress

during my research journey. My sincere thanks also go to the department of Physics and CIFIC, IIT (BHU), Varanasi for availing characterization facilities. I am grateful to all office staffs of the Department and authorities of IIT (BHU), Varanasi for their academic help during this period to complete my research journey.

I acknowledge Inspire Fellowship Department of Science and Technology (DST-INSPIRE), Government of India, for providing junior/senior research fellowship grant.

I would like to thank to my lab mates all the group members of my lab (Luminescent Materials and Devices Development Laboratory) Dr. Santosh Kachhap, Ms. Manisha Sharma, Ms. Shruti, Ms. Shanas Fatima, Mr. Akhil Kumar Rai, Dr. Pradeep Kumar Vishwakarma and Mr. Vimlesh Yadav for helping me in my research work. I would like to express my thanks to all my batchmates (July 2019) and friends for making this journey joyful.

Date: 26.12.2024

Place: Varanasi

(Sachin Singh)

INDEX

CONTENT	PAGES
CERTIFICATE.....	i
DECLARATION BY THE CANDIDATE	iii
COPYRIGHT TRANSFER CERTIFICATE	v
ACKNOWLEDGEMENTS.....	vii
INDEX.....	ix
LIST OF FIGURES	xiii
LIST OF TABLES.....	xix
LIST OF ABBREVIATIONS.....	xxi
PREFACE.....	xxv
Chapter 1 : Introduction.....	1
1.1 Motivation.....	1
1.2 Brief History of Luminescence	2
1.3 Scientific Advances and the Role of Phosphors	3
1.4 Overview of Rare-earth elements.....	8
1.4.1 Distinguished Characteristics of Lanthanides:	10
1.4.2 Spectroscopy of Lanthanides	13
1.5 Lanthanides activated luminescent materials.....	24
1.5.1 Multi-phonon Relaxation in Solids.....	27
1.5.2 Concentration Quenching	28
1.6 Introduction to Upconverting Nanoparticles (UCNPs).....	29
1.7 Characterization of Calcium Molybdate [CaMoO ₄] as a Host Material	31
1.8 Application of Ln ³⁺ activated CaMoO ₄ phosphors	36

1.8.1	Temperature sensing.....	38
1.8.2	LFP Detection Using Luminescent Materials through Powder Dusting method	45
1.9	Conclusion	50
1.10	Organization of the thesis	51
Chapter 2	: Synthesis and Characterization Techniques	55
2.1	Overview.....	55
2.2	Materials Used	56
2.3	Synthesis Techniques.....	56
2.3.1	Solid State Reaction Method.....	57
2.3.2	Sol-Gel Combustion Method.....	59
2.3.3	Hydrothermal method.....	62
2.4	Instrumentation used in present thesis	64
2.4.1	X-ray Diffraction (XRD).....	65
2.4.2	Morphological Analysis	68
2.4.3	Spectroscopic Methods for Material Characterization	72
2.5	Software Relevance in Scientific Research and Analysis	83
2.5.1	Fullprof Suite for XRD Analysis.....	83
2.5.2	ImageJ for TEM and Image Processing	84
2.5.3	Origin Pro 2021	84
2.5.4	Colour Calculator v7.77 for Spectrum Colour Calculation.....	85
Chapter 3	: Structural, Optical, and Temperature Sensing Comparison of Er ³⁺ /Yb ³⁺ co- doped CaMoO ₄ phosphors in bulk and nanostructure forms.....	87
3.1	Introduction.....	87
3.2	Synthesis	89
3.2.1	Solid-state reaction synthesis	89
3.2.2	Combustion synthesis.....	89
3.3	Results and Discussion	90
3.3.1	X-ray diffraction and TEM/SEM measurement: Phase and structure analysis	90

3.3.2	FTIR and Raman measurements: Vibrations and lattice phonon frequency analysis	94
3.4	Luminescence studies	96
3.4.1	Photo-luminescence excitation and emission	96
3.4.2	Photon upconversion emission	97
3.5	Temperature-dependent up-conversion: Optical temperature sensing application	101
3.6	Conclusions	105
Chapter 4	: Bi ³⁺ co-doping in Er ³⁺ /Yb ³⁺ : CaMoO ₄ phosphor for improved upconversion intensity and temperature sensing performance.....	107
4.1	Introduction	107
4.2	Synthesis	109
4.3	Results and discussion	110
4.3.1	X-ray diffraction measurement.....	110
4.3.2	Rietveld refinement analysis.....	113
4.4	SEM and EDS measurements: Surface morphology and elemental analysis	116
4.5	Optical properties	117
4.5.1	FTIR and UV-vis absorption measurement analysis	117
4.5.2	Upconversion spectra analysis.....	119
4.5.3	Chromaticity coordinate analysis.....	121
4.6	Temperature dependent UC measurement: Optical temperature sensing application	122
4.7	Conclusion	126
Chapter 5	: NTCL-Based Temperature Sensing and LFP Visualization Using CaMoO ₄ : Ho ³⁺ /Tm ³⁺ /Yb ³⁺ Phosphors.....	127
5.1	Introduction	127
5.2	Synthesis procedure	129
5.3	Result and discussions	130
5.3.1	Phase, particle shape/size, and elemental mapping analysis	130
5.3.2	Vibrational mode analysis	137
5.3.3	UV-Visible-NIR absorption and bandgap analysis	138

5.3.4	Infrared to visible Upconversion emission analysis	140
5.4	Multifunctional behaviour of CMOHTY phosphor	143
5.4.1	Temperature Sensing application	143
5.4.2	Latent Fingerprints (LFPs)	149
5.5	Conclusion	152
Chapter 6	: Conclusions and Future Perspective.....	153
6.1	Conclusion of the Present Investigation	153
6.2	Future Work	153
6.2.1	Development of Hybrid Materials for Advanced Applications	154
6.2.2	Enhancing Luminescent Properties through Novel Strategies	154
References.....		155
List of Publications.....		1171
Conference/Workshop Attended during PhD.....		173

LIST OF FIGURES

Figure 1.1 Periodic table of elements showing the position of lanthanides	9
Figure 1.2 The list of possible splitting of lanthanides (Ln^{3+}) energy levels.	16
Figure 1.3 Schematic energy level diagram representing the downshifting and the Quantum Cutting process.	20
Figure 1.4 Various energy transfer mechanisms (a) Ground/Excited State Absorption (GSA/ESA), (b) Energy Transfer Upconversion (ETU), (c) Cooperative Energy Transfer (CET). (d) Photon Avalanche (PA)	22
Figure 1.5 General strategies to achieve the high efficiency of UCNPs	30
Figure 1.6 Schematic illustrating the crystal structure of tetragonal CaMoO_4	32
Figure 1.7 The PLE and PL spectrum of CaMoO_4 Phosphor.	35
Figure 1.8 Schematic diagram showing TCLs based thermalization process.	41
Figure 1.9 Fingerprint features (a) Level 1, (b) Level 2, (c) Level 3	48
Figure 1.10 General procedure to reveal fingerprints on any surface	48
Figure 2.1 Solid-state synthesis procedure for sample preparation, including mixing of precursor powders, calcination in furnace, and post-synthesis grinding to achieve uniform particle distribution.	58
Figure 2.2 Sol-gel synthesis procedure for sample preparation, including sol formation, gelation, thermal decomposition (combustion), and post-synthesis grinding for uniform particle distribution.	60
Figure 2.3 Schematic of the hydrothermal synthesis of phosphors, including precursor preparation, autoclave reaction, and post-synthesis cooling, washing, and drying.	62
Figure 2.4 (a) Illustrates the fundamental mechanism of X-ray diffraction, where incident X-rays are reflected off consecutive lattice planes, generating interference patterns unique to each material. (b) X-ray diffractometer (MiniFlex 600, Rigaku, Japan), CIF IIT (BHU).	66

Figure 2.5 (a) Schematic diagram of the instrumental set up of Field emission scanning electron microscope (FE-SEM). (b) Digital photograph of the EVO – SEM MA15 / 18, CARL ZEISS (CIF, IIT BHU).	69
Figure 2.6 (a) Schematic diagram of instrumental set up of Transmission Electron Microscopy (TEM). (b) Digital photograph of Tecnai G2 20 TWIN, HR-TEM setup (CIF IIT BHU).	71
Figure 2.7 (a) Ray diagram of FT-IR spectroscopy. (b) Digital photograph of Nicolet iS5, Thermofisher (CIF, IIT BHU).	73
Figure 2.8 (a) Possible energy diagrams of Rayleigh and Raman scattering process. (b) Digital photograph of Raman setup DXRxi, Thermo Scientific (Department of Physics, Banasthali Vidyapith, Jaipur).	75
Figure 2.9 (a) Ray-diagram of the UV-visible absorption analysis. (b) Digital photograph of JASCO V770 UV-Visible spectrophotometer (Department of Physics, IIT BHU).	77
Figure 2.10 (a) A schematic of the PL spectrophotometer setup. (b) Digital photograph of Horiba Fluorolog-3 spectrophotometer (Department of Physics, IIT BHU).	80
Figure 3.1 (a) XRD pattern of CCEY, SCEY and SCM, and (b) Le-bail fit of SCM.	92
Figure 3.2 TEM image of (a) SCEY, and (b) CCEY. Elemental mapping of (c) SCEY, and (d) CCEY.	93
Figure 3.3 Fourier transforms infrared spectrum for (a) SCM, (b) SCEY, and (c) CCEY.	94
Figure 3.4 Raman spectrum of CaMoO ₄ powder sample synthesized by solid state reaction method.	96
Figure 3.5 (a) excitation spectra, and (b) emission spectra of SCM, SCEY, and CCEY samples.	97
Figure 3.6 (a) UC luminescence spectra of SCEY with a variation in the concentration of Er ³⁺ . (b) comparison of UC emission spectra of SCEY and CCEY. Log-log plot of UC emission intensity vs. laser input power for (c) SCEY, and (d) CCEY.	99

Figure 3.7 Schematic energy level diagram showing UC mechanism in $\text{Er}^{3+}/\text{Yb}^{3+}$ co-doped CaMoO_4 101

Figure 3.8 (a) Green emission FIR (I_{531}/I_{553}) vs. temperature plot, (b) the \ln FIR (I_{531}/I_{553}) vs. inverse absolute temperature plot of $\text{Er}_{0.01}\text{Yb}_{0.2}\text{Ca}_{0.79}\text{MoO}_4$ synthesized by the solid-state method (the UC spectra of the green band at 348 K and 498 K are shown in inset). (c) The plot of relative sensitivity and absolute sensitivity as a function of the temperature of $\text{Er}_{0.01}\text{Yb}_{0.2}\text{Ca}_{0.79}\text{MoO}_4$ synthesized by the solid-state method..... 103

Figure 3.9 (a) Green emission FIR (I_{531}/I_{553}) vs. temperature plot, (b) the \ln FIR (I_{531}/I_{553}) vs. inverse absolute temperature plot of $\text{Er}_{0.01}\text{Yb}_{0.2}\text{Ca}_{0.79}\text{MoO}_4$ synthesized by the gel-combustion method (the UC spectra of the green band at 348 K and 498 K are shown in inset). (c) The plot of relative sensitivity and absolute sensitivity as a function of the temperature of $\text{Er}_{0.01}\text{Yb}_{0.2}\text{Ca}_{0.79}\text{MoO}_4$ synthesized by the gel-combustion method 104

Figure 4.1 (a) XRD patterns of $\text{Ca}_{0.79-x}\text{Bi}_x\text{Er}_{0.01}\text{Yb}_{0.2}\text{MoO}_4$ ($x=0.00, 0.02, 0.05, 0.08, 0.11,$ and 0.14) powder samples. (b) Expanded XRD patterns of $\text{Ca}_{0.79-x}\text{Bi}_x\text{Er}_{0.01}\text{Yb}_{0.2}\text{MoO}_4$ ($x= 0.0, 0.02, 0.05, 0.08, 0.11,$ and 0.14) powder samples between 2θ angle 28.7 to 29.0 degree. Rietveld refined XRD patterns of (c) $\text{Ca}_{0.79}\text{Er}_{0.01}\text{Yb}_{0.2}\text{MoO}_4$, and (d) $\text{Ca}_{0.68}\text{Bi}_{0.11}\text{Er}_{0.01}\text{Yb}_{0.2}\text{MoO}_4$ powder samples..... 111

Figure 4.2 Tetragonal crystal structure of $\text{Ca}_{0.79}\text{Er}_{0.01}\text{Yb}_{0.2}\text{MoO}_4$ in two different orientation obtained after Rietveld refinement of the XRD patterns. 114

Figure 4.3 SEM image of (a) $\text{Ca}_{0.79}\text{Er}_{0.01}\text{Yb}_{0.2}\text{MoO}_4$ (CMEY) and (b) $\text{Ca}_{0.68}\text{Bi}_{0.11}\text{Er}_{0.01}\text{Yb}_{0.2}\text{MoO}_4$ (CMBEY) phosphors. The EDS spectra of (c) CMEY (d) CMBEY phosphors..... 117

Figure 4.4 (a) Fourier transform infrared spectra of CMEY and CMBEY samples. UV-Vis-NIR absorption spectrum of (b) CMEY, and (c) CMBEY phosphors. Tauc plots of the respective UV-visible absorption spectra are provided as insets of the corresponding figures. 118

Figure 4.5 (a) UC emission of powder samples of $\text{Ca}_{0.79-x}\text{Bi}_x\text{Er}_{0.01}\text{Yb}_{0.2}\text{MoO}_4$, with varying Bi concentrations ($x=0.00, 0.02, 0.05, 0.08, 0.11,$ and 0.14), (b) comparison of the UC

emission spectra of CMEY and CMBEY samples both using 980 nm laser as excitation source.....	121
Figure 4.6 Zoomed-in version of the CIE chromaticity diagram for the UC emission of $\text{Ca}_{0.79}\text{Er}_{0.01}\text{Yb}_{0.2}\text{MoO}_4$ (#1), $\text{Ca}_{0.77}\text{Bi}_{0.02}\text{Er}_{0.01}\text{Yb}_{0.2}\text{MoO}_4$ (#2), $\text{Ca}_{0.74}\text{Bi}_{0.05}\text{Er}_{0.01}\text{Yb}_{0.2}\text{MoO}_4$ (#3), $\text{Ca}_{0.71}\text{Bi}_{0.08}\text{Er}_{0.01}\text{Yb}_{0.2}\text{MoO}_4$ (#4), $\text{Ca}_{0.68}\text{Bi}_{0.11}\text{Er}_{0.01}\text{Yb}_{0.2}\text{MoO}_4$ (#5), and $\text{Ca}_{0.65}\text{Bi}_{0.14}\text{Er}_{0.01}\text{Yb}_{0.2}\text{MoO}_4$ (#6) phosphor samples under 980 nm laser excitation. The inset displays the CIE chromaticity diagram for all six samples without zooming.....	122
Figure 4.7 Upconversion spectra of (a) $\text{Ca}_{0.68}\text{Er}_{0.01}\text{Yb}_{0.2}\text{MoO}_4$ and (d) $\text{Ca}_{0.68}\text{Bi}_{0.11}\text{Er}_{0.01}\text{Yb}_{0.2}\text{MoO}_4$ phosphor samples at different temperatures. The logarithm of the FIR as a function of the inverse temperature for (b) $\text{Ca}_{0.68}\text{Er}_{0.01}\text{Yb}_{0.2}\text{MoO}_4$, and (e) $\text{Ca}_{0.68}\text{Bi}_{0.11}\text{Er}_{0.01}\text{Yb}_{0.2}\text{MoO}_4$. The relative and absolute sensitivity for (c) $\text{Ca}_{0.68}\text{Er}_{0.01}\text{Yb}_{0.2}\text{MoO}_4$ and (f) $\text{Ca}_{0.68}\text{Bi}_{0.11}\text{Er}_{0.01}\text{Yb}_{0.2}\text{MoO}_4$ samples, respectively.....	124
Figure 5.1 (a) X-ray diffraction patterns of pristine CMO, CMOHY, CMOTY, and CMOHTY phosphors materials sintered at 750°C, (b) Tetragonal crystalline lattice of CaMoO_4	132
Figure 5.2 Rietveld refinement of XRD plots of CMO, CMOHY, CMOTY, and CMOHTY phosphors.....	133
Figure 5.3 SEM images of (a) CMO, (b) CMOHY, (c) CMOTY, and (d) CMOHTY phosphors sample along with EDAX analysis (in bottom of respective micrograph) with particle size distribution plots (as inset).	135
Figure 5.4 Elemental mapping of a selected region of the CMOHTY phosphor sample. ..	135
Figure 5.5 (a-b) TEM images of optimized CMOHTY phosphors at varying resolutions, (c) Interference fringes of the [112] lattice plane, (d) SAED pattern.	136
Figure 5.6 FTIR spectra (transmittance mode) of (a) CMO, (b) CMOHY, (c) CMOTY and (d) CMOHTY phosphors sintered at 750 °C.....	137
Figure 5.7 (a) UV-Vis absorption spectra of CMO, CMOHY, CMOTY, and CMOHTY phosphor materials. (b) Tauc plot illustrating the bandgap of the same materials.....	139

Figure 5.8 (a) Upconversion spectra of the optimized CMOHY, CMOTY, and CMOHTY phosphor materials. (b) Ln-Ln plot corresponding to different emitting bands under 980 nm excitation.....	141
Figure 5.9 Schematic energy level diagram of Ho ³⁺ /Tm ³⁺ /Yb ³⁺ ions with potential UC mechanisms.....	141
Figure 5.10 Decay time analysis of different emitting bands i.e., (a-b) CMOHY (Ho ³⁺ λ _{emi} =545 nm, 655 nm) and (c-d) CMOTY (λ _{emi} =473 nm, 795 nm), (e-f) CMOHTY (λ _{emi} =545 nm, 655 nm) and (g-h) (λ _{emi} =473 nm, 795 nm) under 980 nm excitation.	142
Figure 5.11 Temperature-dependent UC emission of CMOHTY phosphors under 980 nm excitation.....	144
Figure 5.12 FIR vs Temperature plots fitted with a Boltzmann sigmoidal function of different sets of NTCLs: (a) I ₇₉₅ /I ₄₇₃ , (b) I ₆₈₈ /I ₄₇₃ , (c) I ₆₈₈ /I ₆₅₅ , and (d) I ₆₈₈ /I ₇₉₅ of CMOHTY phosphors sample.	148
Figure 5.13 Relative (S _r) and absolute sensitivity (S _a) plots for different sets of NTCLs, fitted to Boltzmann sigmoidal function.....	148
Figure 5.14 (a-c) Coloured LFP images were acquired using CMOHTY powder phosphors dusted over a glass plate substrate under 980 nm excitation, utilizing filters and high-resolution images of the green LFPs with various minutiae.....	150

LIST OF TABLES

Table 1.1 Early milestones in the discovery of luminescent materials and devices.	4
Table 1.2 List of the rare-earth element's discovery in chronological order.....	9
Table 1.3 List of lanthanide ions, atomic number, radii, electronic configuration, and ground state.	12
Table 1.4 Selection rules for intra 4f-4f transitions for REs ions.	16
Table 1.5 Energy of the maximum phonon frequency for different hosts.	33
Table 2.1 Specifications of Materials Used in Synthesis, Including Chemical Names, Formulas, Purities, and Manufacturers.	56
Table 3.1 The unit cell parameters of CaMoO ₄ powder (SCM) obtained by Le-bail fitting..	92
Table 4.1 Rietveld refined structure parameters of the Ca _{0.79} Er _{0.01} Yb _{0.2} MoO ₄ and Ca _{0.68} Bi _{0.11} Er _{0.01} Yb _{0.2} MoO ₄ powder samples.....	113
Table 4.2 The bond length and angle in Ca, Mo and O-atoms obtained after the Rietveld refinement of the XRD Patterns of Ca _{0.79} Er _{0.01} Yb _{0.2} MoO ₄ and Ca _{0.68} Bi _{0.11} Er _{0.01} Yb _{0.2} MoO ₄ powder samples.....	114
Table 5.1 List of refined structural parameters and residuals of refinements of four different powder samples: CMO, CMOHY, CMOTY, and CMOTHY, as determined by Rietveld analysis.....	133
Table 5.2 Comparison of temperature sensing characteristics based on FIR technique using NTCLs of Ho ³⁺ /Tm ³⁺ in various hosts with the involved transition.....	149

LIST OF ABBREVIATIONS

Å	Angstrom
CBM	Conduction Band Minimum
CCT	Color Correlated Temperature
CIE	Commission International de l'Eclairag
cm	Centimeter
CP	Color Purity
CM	CaMoO ₄
CTB	Charge Transfer Band
DC	Down conversion
DI	Deionized
DMF	Dimethylformamide
DSC	Differential Scanning Calorimetric
EDX	Energy Dispersive X-Ray Analysis
E _g	Band Gap
EOH	Ethanol
Er	Erbium
ESA	Excited State Absorption
Eu	Europium
eV	Electron volt
FIR	Fluorescence Intensity Ratio
FT-IR	Fourier transform Infrared

FWHM	Full width at half maximum
g	Gram
GSA	Ground State Absorption
h	Hour
Ho	Holmium
HR-TEM	High Resolution Transmission Electron Microscope
$h\nu$	Photon Energy
ICDD	International Center for Diffraction Data
JCPDS	Joint Committee on Powder Diffraction Standards
K	Kelvin
LED	Light Emitting Diode
LER	Luminous Efficacy of Radiation
lm/W	Lumens per watt
Ln	Lanthanide
meV	Mili Electron Volt
mg	milligram
min	Minute
ml	Mililiter
MOF	Metal Organic framework
N	Avogadro's number
NCs	Nanocrystals
NIR	Near infrared

nm	Nanometer
NPs	Nanoparticles
ns	Nanosecond
OA	Oleic acid
OAm	Oleylamine
ODE	Octadecene
PL	Photoluminescence
PLE	Photoluminescence Excitation
PLQYs	Photoluminescence Quantum Yields
PMT	Photomultiplier tube
QDs	Quantum dots
R_{exp}	Expected profile residual
R_p	Profile residual
rpm	Round per minute
R_{wp}	Weighted profile residual
s	Second
SEM	Scanning Electron microscope
SSR	Solid State Reaction
T	Temperature
Tm	Thulium
UC	Upconversion
UV-Vis	Ultraviolet-Visible

VBM	Valence Band Maximum
W/m ²	Watt per meter square
WLED	White Light Emitting Diode
XPS	X-Ray Photoelectron Spectroscopy
XRD	X-ray Diffraction
Yb	Ytterbium
S_a	Absolute sensitivity
S_r	Relative sensitivity
k_b	Boltzmann Constant
λ_d	Dominant wavelength
λ_{em}	Emission wavelength
λ_{ex}	Excitation wavelength
τ_{av}	Average decay time
ΔE	Energy separation
°C	Degree Celsius
μm	Micro-meter

PREFACE

Luminescent materials, commonly referred to as phosphors, have garnered significant attention in scientific research due to their extensive applicability in diverse fields such as lighting, sensors, solar cells, and biomedical imaging. Phosphors are typically composed of a crystalline or amorphous host lattice embedded with specific dopants. These dopants introduce additional energy levels into the host lattice, enabling tailored emission properties for targeted applications. Among various dopants, lanthanide (Ln^{3+}) ions stand out for their unique optical properties, including upconversion and downconversion luminescence. Their well-shielded 4f transitions, combined with long luminescence lifetimes, high photostability, and sensitivity to environmental factors, make lanthanides invaluable in advanced optical materials.

Phosphors have been developed using various host lattices, such as phosphates, borates, vanadates, tungstates, molybdates, and garnets. Each host exhibits distinct structural, thermal, and chemical properties that influence luminescence performance. Among these, molybdate-based hosts like CaMoO_4 (calcium molybdate) have emerged as exceptional candidates, particularly for optical temperature sensing and latent fingerprint detection. The tetragonal scheelite structure of CaMoO_4 , with its low phonon energy and broad energy bandgap, offers high thermal and chemical stability, making it suitable for lanthanide doping.

The present thesis focuses on exploring lanthanide-doped CaMoO_4 optical materials for dual applications: contactless temperature sensing and latent fingerprint detection. Optical temperature sensing utilizing thermally coupled and non-thermally coupled levels in lanthanide-doped phosphors is a promising alternative to traditional methods, offering

advantages such as non-invasive measurement, high sensitivity, and operation over a broad temperature range. Lanthanide ions, such as Er^{3+} , Ho^{3+} , Tm^{3+} , and Yb^{3+} , embedded in the CaMoO_4 host, enable precise temperature sensing through their unique luminescent responses to temperature variations. Additionally, this thesis explores the use of upconversion luminescence properties of lanthanide-doped CaMoO_4 for latent fingerprint detection, a critical aspect of forensic science. These materials convert near-infrared excitation into visible light, producing vibrant, high-contrast images of latent fingerprints on various substrates. This technique addresses challenges associated with traditional fingerprint detection methods, such as low visibility and poor contrast on complex backgrounds, by leveraging the color-tunable and dual-mode emission properties of the doped CaMoO_4 phosphors.

The findings of this thesis contribute to the broader understanding of CaMoO_4 as a versatile optical material, advancing its potential for practical applications in both temperature sensing and forensic imaging. Through a combination of material synthesis, advanced characterization techniques, and application-specific investigations, this work lays the groundwork for the development of next-generation luminescent materials. Detailed synthesis procedures and characterization techniques are discussed in Chapter 2. The thesis is divided into six Chapters. The brief explanation of each Chapter is given below:

Chapter 1 introduces the foundational concepts, providing a historical overview of luminescent materials and the evolution of phosphors. The role of lanthanides in optical applications is discussed, with a focus on their unique spectroscopic properties and emission mechanisms. The chapter also examines the structural and optical characteristics of the CaMoO_4 host, highlighting its suitability for lanthanide doping. Applications in optical

thermometry and latent fingerprint detection are introduced, establishing the motivation and scope of the research.

Chapter 2 details the synthesis and characterization techniques used in this thesis. A comprehensive description of the hydrothermal, solid-state, and sol-gel combustion methods employed to prepare lanthanide-doped CaMoO_4 phosphors is provided. Characterization techniques of phosphor materials such as X-ray Diffraction (XRD), Scanning Electron Microscopy (SEM), Transmission Electron Microscopy (TEM), Raman spectroscopy, and photoluminescence analysis are discussed in detail by including their working phenomenon. Additionally, the software used for the data analysis named FullProf, ImageJ, color calculator CIE 1931, and OriginPro 9.0, etc., are briefed.

Chapter 3 investigates and compare the temperature sensing capabilities of $\text{Er}^{3+}/\text{Yb}^{3+}$ doped CaMoO_4 phosphors in both bulk and nanoparticle forms. This chapter also discussed the detailed structural and optical characterization of pristine CaMoO_4 and $\text{Er}^{3+}/\text{Yb}^{3+}$ doped CaMoO_4 phosphors. The results reveal enhanced temperature sensitivity in the nanoparticle-based samples, attributed to their reduced particle size and improved energy transfer efficiency. The chapter demonstrates the potential of nanoscale CaMoO_4 materials in developing high-sensitivity optical thermometers.

Chapter 4 explores the impact of Bi^{3+} co-doping on the temperature sensing performance of $\text{Er}^{3+}/\text{Yb}^{3+}$ doped CaMoO_4 phosphors. The reitveld refinement of optimised $\text{Er}^{3+}/\text{Yb}^{3+}$ doped CaMoO_4 and $\text{Bi}^{3+}/\text{Er}^{3+}/\text{Yb}^{3+}$ doped CaMoO_4 has been done for the detailed structural analysis. The addition of Bi^{3+} ions introduces structural asymmetry, enhancing upconversion emission and temperature sensitivity. The findings highlight the role of co-

doping in optimizing the luminescent properties of CaMoO₄ phosphors for advanced sensing applications.

Chapter 5 focuses on the multifunctionality of CaMoO₄: Ho³⁺/Tm³⁺/Yb³⁺ phosphors, demonstrating their applicability in non-thermally coupled level (NTCL)-based temperature sensing and latent fingerprint visualization. The chapter highlights the high sensitivity and color-tunable emissions of these materials, which enable precise temperature sensing and high-contrast fingerprint imaging under near-infrared excitation.

Chapter 6 consolidates the findings of the thesis, emphasizing the adaptability of CaMoO₄ as a robust host matrix for functional lanthanide doping. The chapter discusses the broader implications of the research and proposes future directions, including the optimization of material properties and exploration of additional applications in emerging optical technologies.

This thesis advances the understanding of lanthanide-doped CaMoO₄ materials and underscores their potential in addressing challenges in temperature sensing and forensic science. I hope this thesis inspires further research in the field of optical materials and their interdisciplinary applications.